MJFAS
Malaysian Journal of Fundamental and Applied Sciences

Abdullah *et al.* | Malaysian Journal of Fundamental and Applied Sciences, Vol. 21 (2025) 2314–2322

RESEARCH ARTICLE

A Molecular Docking Study on Anti-cariogenic Properties of Theaflavins against *Streptococcus mutans*

Muhammad Rizwan Shah Abdullah[a], Anis Fadhlina[a]*, Hassan Ibrahim Sheikh[b], Nur Iman Alia Baharuddin[a], Nur Hazirah Rosli[a], Khairul Bariyyah Abd Halim[c]

[a]Department of Fundamental Dental and Medical Sciences, Kulliyyah of Dentistry, International Islamic University Malaysia, 25200 Kuantan, Pahang, Malaysia; [b]Faculty of Fisheries and Food Science, Universiti Malaysia Terengganu, 21030 Kuala Nerus, Terengganu, Malaysia; [c]Department of Biotechnology, Kulliyyah of Science, International Islamic University Malaysia, 25200 Kuantan, Pahang, Malaysia

Abstract Early childhood caries (ECC) is an aggressive manifestation of dental decay, linked to high levels of *Streptococcus mutans* in dental plaque. In Malaysia, over 70% of children suffer from ECC, leading to premature tooth loss, malnutrition, and reduced quality of life. Common dental-care ingredients like triclosan and triclocarban pose health risks, necessitating safer alternatives. Theaflavins, bioactive compounds in black tea, show potential as natural antimicrobial agents. However, the precise molecular interactions of theaflavins with key virulence-associated proteins of *S. mutans* remain underexplored. This study aims to investigate the antibacterial mechanisms of theaflavins against *S. mutans* using in-silico methods. PyRx was used to evaluate the binding affinities of four selected compounds, theaflavin (TF1), theaflavin-3-gallate (TF2A), theaflavin-3'-gallate (TF2B), and theaflavin-3,3'-digallate (TF3), against seven *S. mutans* proteins (PDB 4TQX: Sortase A, PDB 6CAM: Glucan binding protein, PDB 3QE5: Cell surface protein, PDB 3VX4: Quorum sensing, PDB 3AIC: Glucosyltransferase, PDB 2W3Z: Immune evasion, PDB 3CZC: Carbohydrate uptake). All the ligands were prepared and optimised using Avogadro-1.2 prior to the molecular docking. BIOVIA Discovery visualizer was used to observe the protein-ligand interactions. Findings indicated that theaflavins exhibit significant binding affinities to various *S. mutans* proteins. Among all tested compounds, TF3 demonstrated the strongest binding affinities and favourable hydrogen bonding, particularly against glucan binding protein and glucosyltransferase. These results suggest that TF3 may serve as a promising lead compound for developing natural anti-caries therapeutics targeting *S. mutans* virulence mechanisms.

Keywords: Theaflavins, early childhood caries, anti-cariogenic, *Streptococcus mutans*, molecular docking.

***For correspondence:**
anis_fadhlina@iium.edu.my

Received: 25 Sept. 2024
Accepted: 11 June 2025

Introduction

Early childhood caries (ECC) is characterized by the presence of one or more decaying, missing, or filled tooth surfaces in any primary tooth in a child aged 71 months or less. *Streptococcus mutans* is widely known for its established role in caries aetiology. This oral health issue is particularly significant in underprivileged communities, both in developing and industrialized countries, where malnutrition is prevalent [1]. Despite advances in dental education and oral hygiene awareness, dental caries remains a serious public health challenge, with current global research indicating an increase in caries prevalence [2].

Untreated dental decay can cause discomfort and adversely affect both nutritional status and physical development. ECC is a major public health concern in Malaysia, affecting 75% of preschool children and leaving a significant proportion untreated [3]. The most recent national epidemiological survey in 2015 found a caries prevalence of 71% among Malaysian preschool children. The challenges posed by COVID-19 have further complicated ECC monitoring, leading to the launch of the Gigiku Sihat mobile app [4].

In terms of infectious agents, a study involving 120 Malaysian children aged <6 years found that more than half of the children (55%) tested positive for *S. mutans*. ECC-affected children showed significantly higher counts of *S. mutans* compared to caries-free children. The prevalence of *S. mutans* in ECC children was notably high at 91%, while only 9% was recorded in caries-free children, indicating the significant association of *S. mutans* in Malaysian children with ECC [5].

Currently, various antimicrobial agents, including sodium fluoride, chlorhexidine, and stannous ions, are utilized for preventing and treating dental caries [6-7]. Other antimicrobial compounds include triclosan (TCS) and triclocarban (TCC), which are the most often used antibacterial components in oral care products [8]. Nonetheless, deleterious consequences from the use of these antimicrobial ingredients have been documented. Excessive fluoride use has been linked to fluorosis, restricting its widespread utilisation [9]. TCS exposure has also been associated to neurodevelopmental problems, metabolic abnormalities, and cardiovascular damage [10]. Furthermore, concerns are increasing on the extensive use of broad-spectrum antimicrobial drugs, which contributes to antimicrobial resistance [11].

Consequently, researchers worldwide are turning their attention to alternative ingredients [12]. Research on preventing dental caries has been done using tea extracts to inhibit the growth of cariogenic bacteria. Theaflavins, prominent bioactive compounds in black tea, show promising antimicrobial properties particularly theaflavin-3,3′-digallate (TF3) [13]. Yet, the specific molecular interactions between theaflavins and *S. mutans* virulence factors remain insufficiently explored.

Molecular docking, a computational technique that predicts the preferred orientation and binding affinity of small molecules to their protein targets, is a valuable tool for elucidating the molecular interactions. It enables *in-silico screening* of ligand interactions with specific microbial proteins, offering insights into their potential as therapeutic agents [11]. Therefore, this study employs molecular docking to investigate the binding interactions of four theaflavin derivatives (TF1, TF2A, TF2B, and TF3) with seven virulence-associated *S. mutans* proteins. By identifying theaflavins-protein interactions with the strongest binding affinities and favourable molecular interactions, this work aims to elucidate their potential as natural inhibitors targeting key pathogenic mechanisms of *S. mutans*.

Materials and Methods

Molecular docking was performed to determine the binding sites and affinity of theaflavins on seven main proteins (Sortase A: PDB 4TQX; Glucan binding protein: PDB 6CAM; Cell surface protein: PDB 3QE5; Quorum sensing: PBD 3VX4; Glucosyltransferase: PDB 3AIC; Immune evading: PDB 2W3Z; Carbohydrate uptake PtxB: PBD 3CZC) linked to anti-*S. mutans* activities. PyRx software (version 0.8) was used for the virtual screening of the ligands and target proteins which integrated AutoDock Vina for the molecular docking. The co-crystalised ligand was docked to its protein respectively as a control except for PDB 2W3Z and 3CZC as these proteins have no co-crystalised ligand bonded. The proteins and compounds were loaded as macromolecules and ligands respectively, which were then converted into pdbqt format. The binding energy and hydrogen bonding were used to analyse the molecular docking output. The results of all possible docked conformations of the ligands were generated and saved in an Excel file. The key parameters such as number of H-bonding and distance between the H-bonded residues of the proteins and ligands were analysed by BIOVIA Discovery Studio [11]. The most favourable binding poses of the ligands were analysed by selecting those with the lowest free energy of binding (ΔG) and the highest number of active residues involved in the H-bonding.

Protein Preparation

All protein/macromolecules used were downloaded in three-dimensional (3D) structure from Protein Data Bank (https://www.rcsb.org/) as PDB files and prepared using BIOVIA Discovery Studio Visualizer. The proteins were prepared by removing water molecules, adding hydrogen (polar), and defining the active site from the co-crystalised ligand prior to removing it [11]. The grid box (XYZ coordinates) for all proteins were determined based on their active site or around their crystal structures (Table 1). Then, the prepared proteins were saved as a PDB file.

Table 1. The coordinates of macromolecules

Macromolecules	Classification	PDB ID	Coordinates		
			X	Y	Z
Sortase A	Hydrolase	4TQX	6.66	28.82	−14.81
Glucan binding protein C	Sugar binding protein	6CAM	238.48	−28.20	3.63
Antigen I/II carboxy-terminus	Adhesin	3QE5	73.86	50.75	130.59
ATP-binding protein ComA	Signaling protein (Quorum sensing)	3VX4	40.67	30.28	8.75
Glucansucrase	Glycosyltransferase	3AIC	193.01	47.23	193.58
CE4 esterase	Hydrolase	2W3Z	40.74	57.74	23.042
PTS IIB(PtxB)	Phosphotransferase	3CZC	9.79	39.59	3.63

Ligand Preparation

All ligands (Figure 1) were downloaded from PubChem library (https://pubchem.ncbi.nlm.nih.gov/) in 3D conformation as SDF files format. Avogadro software was used to prepare and optimise the ligands. The ligand preparation was done by adding hydrogen atom and optimising the ligands' geometry until the structure became static. The prepared ligands were saved as a PDB file.

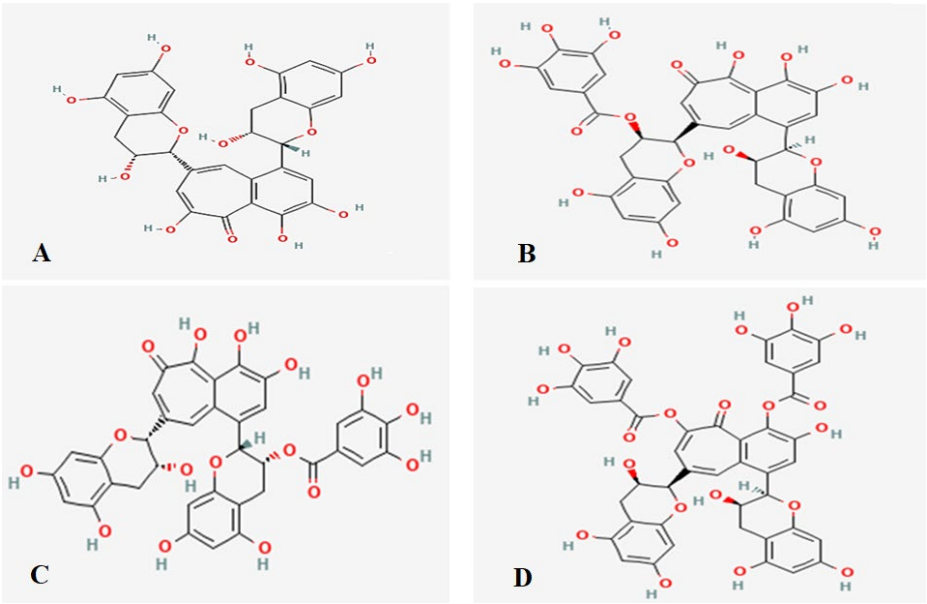

Figure 1. Chemical structure of theaflavins retrieved from PubChem database. A: Theaflavin (TF1), B: Theaflavin-3-gallate (TF2a), C: Theaflavin-3'-gallate (TF2b), D: Theaflavin-3,3'-digallate (TF3)

Results and Discussion

Molecular docking simulation is essential, especially for the screening of potential new drug compounds. The results from our molecular docking simulation of theaflavins with the selected proteins were compared with their known inhibitors or co-crystalised ligands except for 2W3Z and 3CZC, as no co-crystallised ligands were bound to these proteins. Additionally, the molecular docking results were analysed to identify the most promising protein that exhibited the strongest interaction with theaflavins.

Theaflavins (TFs) belong to a class of polyphenolic compounds featuring a benzotropolone skeleton. They impart the brownish pigment to black tea, comprising approximately 2–6% of its dried leaves (*Camellia sinensis*). TFs are produced during the oxidation of specific catechins (epicatechin and epigallocatechin-3-gallate) [14-16]. Fermentation transforms catechins into TFs, primarily theaflavin (TF1), theaflavin-3-gallate (TF2A), theaflavin-3'-gallate (TF2B), theaflavin-3,3'-digallate (TF3), and certain polymers of thearubigin [17]. TFs are potentially valuable for preventing and/or treating the

progression of dental caries. Notably, TFs inhibit the gene expression of glucan binding proteins (Gbps) GbpB and GbpC in *S. mutans* during biofilm formation, influencing bacterial aggregation and playing a crucial role in sucrose-dependent biofilm formation as well as cell shape integrity [18-20]. Upon testing on human lung fibroblast tissue, CEM cells, A549, and Vero cells, TFs were reported to have minimum to no effect on these cells [21]. Among all TFs, TF3 was studied for its biological activities such as antioxidant, anti-inflammatory, anti-microbial, and anti-cancer properties. It was suggested as a potential adjuvant treatment for ovarian cancer by targeting *Chk2* and *p27* [22]. TF3 was also reported to exhibit a potent inhibitory effect on α-hemolysin (Hla) of *Staphylococcus aureus* [23]. Besides, it showed a promising anticariogenic properties by inhibiting the formation of *S. mutans* biofilm without impacting the bacterial growth [24].

In the present study, the molecular docking simulations demonstrated a broad range of binding energies for TF1, TF2a, TF2b, and TF3 against multiple target proteins. The first target, Sortase A (PDB 4TQX), is responsible for bacterial adhesion and biofilm development by anchoring surface proteins to the bacterial cell wall [25]. This mechanism is further mediated by glucan binding protein (GbpC, PDB 6CAM), which aids in the attachment of *S. mutans* to the tooth surface by binding to glucans and thus stabilises the biofilms [26]. Meanwhile, glucosyltransferase (Gtf, PDB 3AIC) is essential for synthesising the glucans [27]. Besides, the cell surface protein PAc (PDB 3QE5) also plays a key role in bacterial adhesion to tooth surfaces by interacting with salivary glycoproteins for colonisation [28].

As for bacterial communication, quorum sensing protein (PDB 3VX4) is responsible for regulating bacterial gene expression based on the bacterial population density, thus ensuring coordinated biofilm formation and virulence factors [29]. In terms of bacterial survival and biofilm maintenance, the immune evasion protein (PDB 2W3Z) helps in the bacterial evasion of host immune defense, and the carbohydrate uptake protein (PDB 3CZC) facilitates the acquisition of essential nutrients [30-31]. Together, these proteins are crucial for bacterial adhesion, biofilm formation, integrity and survival.

The result of molecular docking analysis showed that all binding energy values were negative which indicates the stabilisation of the TFs-protein complexes [32], as presented in Table 2. The strongest binding affinity was exhibited by TF3 against several target proteins, with the lowest binding energy observed against 6CAM (−10.6 kcal/mol). The high affinity of TF3 towards 6CAM may indicate its potential as a potent inhibitor against the glucan binding protein. Meanwhile, the order of binding affinity (6CAM > 3AIC > 2W3Z > 3QE5 > 3VX4> 4TQX > 3CZC) may suggest its favourable binding for certain active sites as well as its specificity towards these proteins.

A recent study [33] highlighted that a strong binding interaction may be indicated by a binding energy of −7 kcal/mol or lower (e.g., −8 or −9 kcal/mol). The binding energy threshold of −7.0 kcal/mol is commonly used to distinguish between strong and weak binders. By this criterion, all TFs demonstrated considerable binding affinity, particularly TF3. For instance, the 6CAM-TF3 complex (Figure 2) surpasses this threshold by a wide margin (−10.6 kcal/mol), indicating a strong and plausible biologically relevant interaction. In contrast, the 3CZC-TF2a complex (−4.8 kcal/mol) displayed the weakest interaction, suggesting a reduced likelihood of inhibitory potential against 3CZC. Furthermore, it is noteworthy that most TFs outperformed the co-crystallised ligands or known inhibitors in terms of their binding energy against targets such as 6CAM, 3QE5, 3VX4, and 3AIC, implying their superior inhibition profiles against these proteins.

Table 2. The binding energy, hydrogen bond formation and interacting residues of all ligands for each protein

PBD 4TQX Active site: Ala139, Cys205, and Arg213			
Ligands	**Binding Energy (kcal/mol)**	**Number of H-bonds**	**H-bonded residues with distance (Å)**
Chalcone	−6.1	0	NA
TF1	−6.1	3	His140 (2.8), Ser148 (2.67)
TF2a	−5.7	5	Thr206 (2.71), Asp207 (2.88 & 2.56), Ala208 (2.22), Val141 (2.75)
TF2b	−6.8	4	His140 (2.50), Met144 (2.43), Gly143 (2.01), Ser147 (2.79)
TF3	−6.2	5	Ser138 (2.17), **Cys205** (3.09), Ala210 (2.68), **Arg213** (2.90, 2.37, 2.56)

PBD 6CAM Active site: Ser347, Asn349, Glu360, and 410-418			
Ligands	**Binding Energy (kcal/mol)**	**Number of H-bonds**	**H-bonded residues with distance (Å)**
β-D-glucopyranose	−5.3	5	**Ser347** (2.27 & 2.95), **Asn349** (1.76), **Glu360** (2.70), Thr449 (2.75)
TF1	−9.5	5	**Ser347** (3.05), His358 (2.91), Asp402 (1.90), Asp408 (2.44), Asn442 (2.69)
TF2a	−9.2	7	**Asn349** (2.94), **Glu360** (2.16), Gln391 (2.00), Gly403 (2.74), Asn442 (2.32), Thr449 (2.28), Trp451 (2.94)
TF2b	−8.7	8	**Ser347** (2.26), **Asn349** (2.70), Trp351 (2.20), **Glu360** (2.59 & 2.82), Gly403 (2.65), Trp451 (2.12 & 2.75)
TF3	−10.6	6	**Ser347** (1.84 & 2.32), **Asn349** (2.82), Thr353 (2.23), **Glu360** (2.60), Thr449 (2.43)
PBD 3QE5 Active site: Gln1024, Gly1055, Asn1076, Ile1157, Asn1320, Gly1321, Ala1323			
Ligands	**Binding Energy (kcal/mol)**	**Number of H-bonds**	**H-bonded residues with distance (Å)**
α-D-glucopyranose	−4.9	6	Tyr1056 (2.17), Phe1058 (2.83), Tyr1074 (2.98), **Asn1076** (2.09, 2.03), Asn1079 (1.77)
TF1	−7.7	4	Asp1115 (1.64), Lys1259 (2.17), Ala1260 (2.47), **Ala1323** (2.74)
TF2a	−6.6	10	Lys1023 (2.09), Leu1113 (2.25), **Gln1024** (2.94), Asn1114 (1.81 & 2.18), Ser1258 (2.48), Lys1259 (2.07), Gly1319 (2.63), **Gly1321** (2.96)
TF2b	−8.1	8	**Gln1024** (2.71, 1.84), Asn1114 (2.07), Aps1115 (1.94 & 2.20), **Ile1157** (2.63), Lys1259 (2.14), **Gly1321** (2.53)
TF3	−8.2	8	**Gln1024** (2.05), Asn1114 (2.12), Gly1144 (2.30), **Ile1157** (2.84), Ala1260 (2.01), Gln1312 (1.93), Tyr1314 (2.88), **Gly1321** (1.89)
PBD 3VX4 Active site: Tyr537, Lys567, Ser666, Asp689, Ala690, His720			
Ligands	**Binding Energy (kcal/mol)**	**Number of H-bonds**	**H-bonded residues with distance (Å)**
Adenosine-5'-Triphosphate	−7.2	11	Asp542 (2.43), Thr543 (2.54), Ala562 (3.09), Gly564 (2.05), Ser565 (2.95), Gly566 (2.07), **Lys567** (2.43), Thr568 (2.10), Thr569 (2.45), Gln609 (2.64), Gln736 (2.41)
TF1	−7.7	5	**Tyr537** (2.38), **Lys567** (2.70), Thr569 (2.48), Lys572 (2.16), Gln609 (2.68)
TF2a	−8.7	5	Ser565 (2.52 & 2.90), Gly566 (1.94), **Lys567** (2.33), **His720** (2.66)
TF2b	−7.9	7	Ala562 (2.91), Gly566 (2.0 & 2.69), **Lys567** (1.99), Thr568 (2.61), Gln609 (2.22 & 2.34)
TF3	−7.6	11	Thr543 (2.08), Ser563 (2.21), Ser565 (2.63), Gly566 (1.72 & 2.81), **Lys567** (2.76), Lys572 (2.52), Gln609 (2.0), **Asp689** (2.28), Gln736 (2.04 & 2.92)
PBD 3AIC Active site: Tyr430, Leu433, Arg475, Asp477, Asn481, Glu515, Trp517, His587, Asp588, Tyr916			
Binding site: PDB 3AIC	**Binding Energy (kcal/mol)**	**Number of H-bonds**	**H-bonded residues with distance (Å)**
Acarbose	−7.8	7	**Tyr430** (2.77), **Asp477** (2.28), **His587** (2.18), **Asp588** (2.78), Gln592 (2.09, 2.36, 2.60)
TF1	−9.9	4	**Asn481** (2.55), **Trp517** (2.86), **Asp588** (2.34), Asp593 (1.98)
TF2a	−9.2	9	Asp424 (1.92), Thr426 (2.90), **Tyr430** (2.18), **Asn481** (2.42), **Trp517** (2.18), Asn537 (2.72), Arg540 (2.21), Asp593 (2.32), Tyr610 (2.80)
TF2b	−10.1	4	**Tyr430** (2.56), Asp593 (1.87), Asp909 (2.33), Lys977 (2.34)
TF3	−10.0	6	Asp380 (2.46), Asp424 (2.61), **Asn481** (2.58), **Trp517** (3.0), Glu590 (2.68), Asp909 (2.64)

PBD 2W3Z Active site: Asp114, Asp115, His166, His 170, Arg211, His281, Trp239, Asp244, Leu279,			
Ligands	**Binding Energy (kcal/mol)**	**Number of H-bonds**	**H-bonded residues with distance (Å)**
TF1	−7.9	2	**Trp239** (2.04), Ala246 (2.29)
TF2a	−7.7	5	**Asp115** (2.0), **His166** (2.68), Tyr172 (2.68), Gly214 (2.14), Glu247 (2.17)
TF2b	−8.9	8	**Asp115** (2.43), Asp118 (2.30), **His170** (2.04 & 2.24), Tyr172 (2.08), Ser284 (2.79), Glu285 (2.52), Lys286 (2.15)
TF3	−9.4	5	Asp118 (2.81), Ser169 (2.44), **His170** (2.21), Glu285 (2.30), Lys286 (2.08)
PBD 3CZC Active site: Cys8, Gly9, Asn10, Gly11, Mse12,13, 14, Ser15, Met66, Pro67, His68			
Ligands	**Binding Energy (kcal/mol)**	**Number of H-bonds**	**H-bonded residues with distance (Å)**
TF1	−5.5	4	**Gly9** (2.73), **Mse12** (2.70), Ser38 (2.60), Glu43 (2.77)
TF2a	−4.8	4	**Asn10** (2.33), **Gly11** (2.76), **Mse12** (2.48), **Ser15** (2.63)
TF2b	−5.2	4	**Cys8** (2.21), **Mse12** (2.96), Ser38 (2.59), Glu43 (2.67)
TF3	−5.7	3	**Gly11** (2.37), **Mse12** (2.02), Ser38 (2.19)

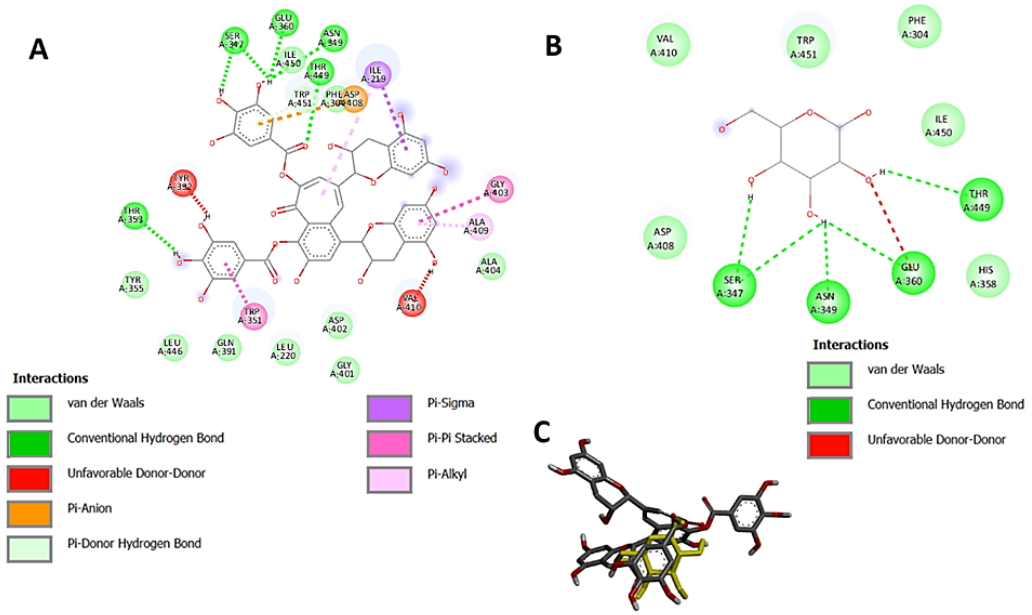

Figure 2. Image A, B, and C show the interactions of TF3, β-D-glucopyranose, and the superimposed structures of TF3 (grey) and β-D-glucopyranose (yellow) within the binding site of 6CAM, respectively

H-bonds play an essential role in establishing the strength and specificity of protein-ligand interactions. Table 2 shows that TF3 forms a higher number of H-bonds with 3VX4 (11 bonds) compared to the other analysed TFs as illustrated in Figure 3. TF3 formed a similar number of H-bonds as the control, Adenosine-5'-Triphosphate, suggesting its comparable activity to the control and potentially an effective inhibitor against this protein. In terms of H-bond distances, the optimum distance ranges from 1.5 to 2.6 Å [32]. H-bonds with a distance greater than 3.0 Å may indicate a weak and readily disturbed interaction. The H-bond distance determines the strength of the interaction whereby the shorter the bond, the stronger the binding affinity and interaction of the protein-ligand complex. Furthermore, a single H-bond can contribute to approximately 20-25 kJ/mol of energy, which enhances the stability of the interaction [32].

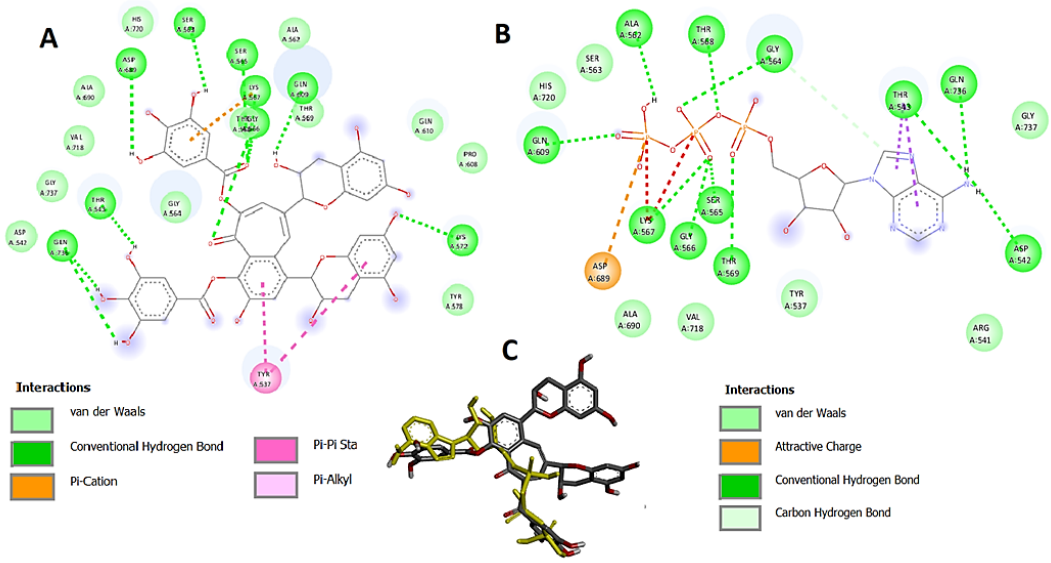

Figure 3. Image A, B, and C show the interactions of TF3, ATP, and the superimposed structure of TF3 (grey) and ATP (yellow) within the binding site of 3VX4, respectively

TF3 consistently formed H-bonds within the favourable range of distances across most proteins. However, the H-bond formed with Cys205 in 4TQX had a distance of 3.09 Å, suggesting a weaker interaction that might be less stable compared to other TFs-protein interactions. Despite this, the overall binding profile of TF3 with 4TQX is reinforced by additional non-covalent interactions (Figure 4), such as van der Waals forces and pi-alkyl interactions, compensating for the weaker H-bonding. TF3 formed H-bonds with active residues of 4TQX (Cys205, Arg213), 6CAM (Ser347, Glu360, Asn349), 3QE5 (Ile1157, Gln1024, Gly1321), 3VX4 (Asp689, Lys567), 3AIC (Trp517, Asn481), 2W3Z (His170), and 3CZC (Mse12, Gly11). This further emphasises the specificity of TF3. These residues are critical for catalytic activity [26, 30, 31,34-36], and their involvement in H-bond formation may suggest that TF3 is capable of interfering with the enzymes function.

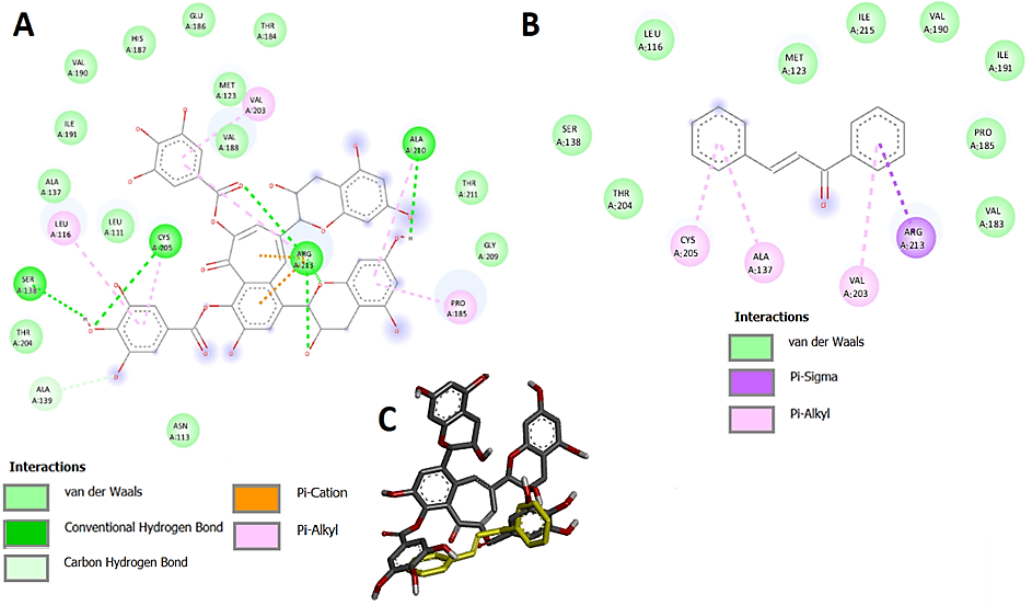

Figure 4. Image A, B, and C show the Interactions of TF3, chalcone, and the superimposed structure of TF3 (grey) and chalcone (yellow) within the binding site of 4TQX, respectively

Given these results, TF3 presents itself as a more promising candidate for further drug development efforts than the current inhibitors in terms of both binding energy and H-bond interactions. TF3 could serve as a lead compound for the development of enzyme inhibitors targeting 6CAM and other proteins. The strong binding interactions observed for TF3 make it a prime candidate for further experimental validation, such as enzyme inhibition assays and in vivo studies. The significant binding energy and number of H-bonds formed with critical residues suggest that TF3 may exhibit broad-spectrum enzyme inhibitory activity, making them useful in the context of multi-target drug design. This could be particularly beneficial in therapeutic areas where multiple pathways contribute to progression such as caries.

Conclusions

This study investigated the antibacterial potential of TFs against *S. mutans*, a key contributor to early childhood caries, using molecular docking. Among the four TFs tested (TF1, TF2a, TF2b, TF3), TF3 demonstrated the strongest binding affinities, particularly against glucan binding protein and glucosyltransferase, with low binding energies indicating stable interactions. TF3's ability to form multiple H-bonds with critical proteins involved in bacterial adhesion and biofilm formation highlights its potential as an effective anti-caries agent. The insights from this study may provide a foundation for future experimental validation and drug design efforts. Further studies are warranted to explore the dynamic interactions between protein and TFs at the atomic level as well as the therapeutic potential of TF3 in the context of enzyme inhibition and multi-target drug development.

Conflicts of Interest

The authors declare that there is no conflict of interest.

Acknowledgement

The authors wish to thank the Ministry of Higher Education (MOHE) Malaysia for the research funding under Fundamental Research Grant Scheme (FRGS) Fasa 1 2024 (FRGS/1/2024/SKK12/UIAM/02/1), and International Islamic University Malaysia for providing the research facilities.

References

[1] Anil, S., & Anand, P. S. (2017). Early childhood caries: Prevalence, risk factors, and prevention. *Frontiers in Pediatrics, 5*, 157.

[2] Dye, B. A., Vargas, C. M., Fryar, C. D., Ramos-Gomez, F., & Isman, R. (2017). Oral health status of children in Los Angeles County and in the United States, 1999–2004. *Community Dentistry and Oral Epidemiology, 45*, 135–144.

[3] Bilal, S., Abdulla, A. M., Andiesta, N. S., Babar, M. G., & Pau, A. (2021). Role of family functioning and health-related quality of life in pre-school children with dental caries: A cross-sectional study. *Health and Quality of Life Outcomes, 19*(1), 1–10.

[4] Akmal Muhamat, N., Hasan, R., Saddki, N., Mohd Arshad, M. R., & Ahmad, M. (2021). Development and usability testing of mobile application on diet and oral health. *PLoS One, 16*(9), e0257035.

[5] Almoudi, M. M., Hussein, A. S., Abu-Hassan, M. I., Saripudin, B., & Mohamad, M. S. F. (2021). The Association of Early Childhood Caries with Salivary Antimicrobial Peptide LL37 and Mutans Streptococci. *Journal of Clinical Pediatric Dentistry, 45*(5), 330–336.

[6] Ferreira-Filho, J. C. C., Marre, A. T. D. O., de Sá Almeida, J. S., Lobo, L. D. A., Farah, A., Romanos, M. T. V., Maia, L. C., Valença, A. M. G., & Fonseca-Gonçalves, A. (2020). Therapeutic potential of bauhinia forficata link in dental biofilm treatment. *Journal of Medicinal Food, 23*(9), 998–1005.

[7] Anderson, A. C., Al-Ahmad, A., Schlueter, N., Frese, C., Hellwig, E., & Binder, N. (2020). Influence of the long-term use of oral hygiene products containing stannous ions on the salivary microbiome–A randomized controlled trial. *Scientific Reports, 10*(1), 9546.

[8] Halden, R. U., Lindeman, A. E., Aiello, A. E., Andrews, D., Arnold, W. A., Fair, P., Fuoco, R. E., Geer, L. A., Johnson, P. I., Lohmann, R., & McNeill, K. (2017). The Florence statement on triclosan and triclocarban. *Environmental Health Perspectives, 125*(6), 064501.

[9] Li, M., Qu, X., Miao, H., Wen, S., Hua, Z., Ma, Z., & He, Z. (2020). Spatial distribution of endemic fluorosis caused by drinking water in a high-fluorine area in Ningxia, China. *Environmental Science and Pollution Research, 27*, 20281–20291.

[10] Alfhili, M. A., & Lee, M. H. (2019). Triclosan: An update on biochemical and molecular mechanisms. *Oxidative Medicine and Cellular Longevity, 2019*(1), 1607304.

[11] Fadhlina, A., Sheikh, H. I., & Lestari, W. (2023). Molecular docking studies of an isolated angucycline of Stereospermum fimbriatum, a novel anti-MRSA agent. *Malaysian Journal of Fundamental and Applied*

Sciences, 19(4), 553–562.
[12] Awang, A. F. I., Taher, M., & Susanti, D. (2016). The mode of antimicrobial action of Cinnamomum burmannii's essential oil & cinnamaldehyde. *Jurnal Teknologi, 78*(11-2).
[13] Luo, Q., Luo, L., Zhao, J., Wang, Y., & Luo, H. (2023). Biological potential and mechanisms of tea's bioactive compounds in tea: An updated review. *Journal of Advanced Research*. Advance online publication.
[14] Friedman, M. (2007). Overview of antibacterial, antitoxin, antiviral, and antifungal activities of tea flavonoids and teas. *Molecular Nutrition & Food Research, 51*, 116–134.
[15] He, H. F. (2017). Research progress on theaflavins: Efficacy, formation, and preparation. *Food & Nutrition Research, 61*, 1344521.
[16] Shan, Z., Nisar, M. F., Li, M., Zhang, C., & Wan, C. C. (2021). Theaflavin chemistry and its health benefits. *Oxidative Medicine and Cellular Longevity, 2021*, 1–16.
[17] Liu, C., Hao, K., Liu, Z., Liu, Z., & Guo, N. (2021). Epigallocatechin gallate (EGCG) attenuates staphylococcal alpha-hemolysin (Hla)-induced NLRP3 inflammasome activation via ROS-MAPK pathways and EGCG-Hla interactions. *International Immunopharmacology, 100*, 108170.
[18] Kong, J., Xia, K., Su, X., Zheng, X., Diao, C., Yang, X., *et al.* (2021). Mechanistic insights into the inhibitory effect of theaflavins on virulence factors production in Streptococcus mutans. *AMB Express, 11*, 102.
[19] Duque, C., Stipp, R. N., Wang, B., Smith, D. J., Höfling, J. F., Kuramitsu, H. K., *et al.* (2011). Downregulation of GbpB, a component of the VicRK regulon, affects biofilm formation and cell surface characteristics of Streptococcus mutans. *Infection and Immunity, 79*, 786–796.
[20] Zhu, M., Ajdić, D., Liu, Y., Lynch, D., Merritt, J., & Banas, J. A. (2009). Role of the Streptococcus mutans irvA gene in GbpC-independent, dextran-dependent aggregation and biofilm formation. *Applied and Environmental Microbiology, 75*, 7037–7043.
[21] Yussof, A., Cammalleri, B., Fayemiwo, O., Lopez, S., & Chu, T. (2022). Antibacterial and sporicidal activity evaluation of theaflavin-3, 3′-digallate. *International Journal of Molecular Sciences, 23*(4), 2153.
[22] Gao, Y., Yin, J., Tu, Y., & Chen, Y. C. (2019). Theaflavin-3, 3′-digallate suppresses human ovarian carcinoma OVCAR-3 cells by regulating the checkpoint kinase 2 and p27 kip1 pathways. *Molecules, 24*(4), 673.
[23] Goc, A., Sumera, W., Rath, M., & Niedzwiecki, A. (2023). Inhibition of α-hemolysin activity of Staphylococcus aureus by theaflavin 3, 3'-digallate. *PLoS One, 18*(8), e0290904.
[24] Wang, S., Wang, Y., Wang, Y., Duan, Z., Ling, Z., Wu, W., Tong, S., Wang, H., & Deng, S. (2019). Theafavin-3,3'-digallate suppresses biofilm formation, acid production, and acid tolerance in Streptococcus mutans by targeting virulence factors. *Frontiers in Microbiology, 10*, 1705.
[25] Wallock-Richards, D. J., Marles-Wright, J., Clarke, D. J., Maitra, A., Dodds, M., Hanley, B., & Campopiano, D. J. (2015). Molecular basis of Streptococcus mutans sortase A inhibition by the flavonoid natural product trans-chalcone. *Chemical Communications, 51*(52), 10483–10485.
[26] Mieher, J. L., Larson, M. R., Schormann, N., Purushotham, S., Wu, R., Rajashankar, K. R., Wu, H., & Deivanayagam, C. (2018). Glucan binding protein C of Streptococcus mutans mediates both sucrose-independent and sucrose-dependent adherence. *Infection and Immunity, 86*(7), e00146-18.
[27] Bowen, W. H., & Koo, H. (2011). Biology of Streptococcus mutans-derived glucosyltransferases: Role in extracellular matrix formation of cariogenic biofilms. *Caries Research, 45*(1), 69–86.
[28] Matsumoto-Nakano, M. (2018). Role of Streptococcus mutans surface proteins for biofilm formation. *Japanese Dental Science Review, 54*(1), 22–29.
[29] Li, Y. H., Tang, N., Aspiras, M. B., Lau, P. C., Lee, J. H., Ellen, R. P., & Cvitkovitch, D. G. (2002). A quorum-sensing signaling system essential for genetic competence in Streptococcus mutans is involved in biofilm formation. *Journal of Bacteriology, 184*(10), 2699–2708.
[30] Deng, D. M., Urch, J. E., ten Cate, J. M., Rao, V. A., van Aalten, D. M., & Crielaard, W. (2009). Streptococcus mutans SMU. 623c codes for a functional, metal-dependent polysaccharide deacetylase that modulates interactions with salivary agglutinin. *Journal of Bacteriology, 191*(1), 394–402.
[31] Lei, J., Li, L. F., & Su, X. D. (2009). Crystal structures of phosphotransferase system enzymes PtxB (IIBAsc) and PtxA (IIAAsc) from Streptococcus mutans. *Journal of Molecular Biology, 386*(2), 465–475.
[32] Haron, N., Nadia, N., Farahin, P. N., Susanti, D., Hasniza, N., Bariyya, K., & Halim, A. (2021). Molecular docking of polyphenol compounds from Anacardium occidentale with alpha-glucosidase and dipeptidyl-peptidase-4 enzymes. *Malaysian Journal of Fundamental and Applied Sciences, 17*, 202–216.
[33] Broni, E., Striegel, A., Ashley, C., Sakyi, P. O., Peracha, S., Velazquez, M., Bebla, K., Sodhi, M., Kwofie, S. K., Ademokunwa, A., & Khan, S. (2023). Molecular docking and dynamics simulation studies predict potential anti-ADAR2 inhibitors: Implications for the treatment of cancer, neurological, immunological and infectious diseases. *International Journal of Molecular Sciences, 24*, 6795.
[34] Luo, H., Liang, D. F., Bao, M. Y., Sun, R., Li, Y. Y., Li, J. Z., Wang, X., Lu, K. M., & Bao, J. K. (2017). In silico identification of potential inhibitors targeting Streptococcus mutans sortase A. *International Journal of Oral Science, 9*(1), 53–62.
[35] Alhobeira, H. A., Al Mogbel, M., Khan, S., Khan, M., Haque, S., Somvanshi, P., Wahid, M., & Mandal, R. K. (2021). Prioritization and characterization of validated biofilm blockers targeting glucosyltransferase C of Streptococcus mutans. *Artificial Cells, Nanomedicine, and Biotechnology, 49*(1), 335–344.
[36] Larson, M. R., Rajashankar, K. R., Crowley, P. J., Kelly, C., Mitchell, T. J., Brady, L. J., & Deivanayagam, C. (2011). Crystal structure of the C-terminal region of Streptococcus mutans antigen I/II and characterization of salivary agglutinin adherence domains. *Journal of Biological Chemistry, 286*(24), 21657–21666.

\